

# Use of Time-Frequency map combined with DBSCAN algorithm for separation of partial discharge pulses under DC voltage

Alessio Di Fatta<sup>1</sup>, Pietro Romano<sup>1</sup>, Antonino Imburgia<sup>1</sup>, Guido Ala<sup>1</sup>, Giuseppe Rizzo<sup>2</sup>, Vincenzo Li Vigni<sup>2</sup>, Marco Albertini<sup>3</sup>, Stefano Franchi Bononi<sup>3</sup>

<sup>1</sup>L.E.PR.E. H.V. Laboratory, Department of Engineering, University of Palermo, Italy;

<sup>2</sup>Prysmian Electronics, Palermo, Italy;

<sup>3</sup>Prysmian Group, Milan, Italy

Corresponding Author: [alessio.difatta@community.unipa.it](mailto:alessio.difatta@community.unipa.it)

**Abstract**—The Phase-Resolved-Partial-Discharge pattern (PRPD) is a conventional technique used for the evaluation of partial discharges (PD) phenomena in High-Voltage-Alternating-Current (HVAC) systems. This map is constructed by plotting the peak of each detected pulses as a function of the phase angle of the supply voltage. Therefore it is obvious that this technique cannot be used for the analysis of data from PD measurement under different supply voltage condition (DC). The aim of this paper is to evaluate the application of the Time-Frequency map (TF map) for the analysis of a dataset obtained from PD measurement under DC voltage. A density-based clustering algorithm was also used to gain more insight from the collected data. The results show that, with this approach, it's possible to perform a noise rejection and identify PD pulses.

**Keywords**—Partial Discharge, PD, Time-Frequency map, Density-Based clustering algorithm.

## I. INTRODUCTION

THE IEC 60270 standard defines partial discharge a “localized electrical discharge that only partially bridges the insulation between conductors and which can or cannot occur adjacent to a conductor”. This phenomenon mainly affects insulation systems characterized by structural defects or discontinuity in the dielectric material. It has long been known in scientific literature that PD causes a slow degradation process of the insulating systems with resulting loss of its dielectric properties, aging, and reduction of component reliability [1, 2]. If no monitoring is performed PD can lead to total discharge and component failure. For these reasons, the PD monitoring is an important tool for assessing the state of an insulation system and to prevent, with appropriate maintenance measures, the failure. The measurement phase is followed by a data analysis phase (post processing) to perform a noise rejection and to separate and identify the different PD types (corona, surface and internal). The technique most used for the analysis of data obtained from AC measurements is the Phase-Resolved-Partial-Discharge pattern that consists in the construction of a two-dimensional map in which the peaks of each detected pulses are plotted as a function of the phase angle of the supply voltage. The growing diffusion of HVDC systems makes necessary the development of analysis techniques also for DC case, for which the PRPD pattern cannot be available due to the constant value of the supply voltage. The degradation phenomena under DC case are different from the AC ones

and influenced by phenomena such as space charge and thermal gradient [3, 4]. No technical standards have been developed for this case, for these reasons different approaches are presented in literature [5, 6]. In this paper a technique based on a statistical approach is evaluated. It is the Time-Frequency map described in detail in section 3 [7, 8]. In section 4 a density-based clustering algorithm, used to make the analysis more complete, is discussed. In section 2 the experimental setup that was used for PD measurement is explained. In the end the results of the performed tests are illustrated.

## II. EXPERIMENTAL SETUP

The data analyzed in this work were obtained through a PD measurement performed with the setup shown in figure 1. This D.U.T. consists in a couple of specimens connected in series. The first one is composed of a pair of electrodes with a XLPE middle layer of 0.5 mm thick. The second one is composed of a pair of electrodes with two XPLE middle layers of 0.3 mm thick. In one of this two layers a void was carried out to favor the occurrence of internal discharges. Both specimens are immersed in mineral oil. Through an HVDC generator several voltage levels were applied. The PD detection has been carried out through a *PRY-CAM*<sup>®</sup> *Portable*, developed by Prysmian Electronics [9]. This detection system is based on wireless technology that employs a special ultra-wide band antenna as a sensor combined with a digital acquisition system with a sampling frequency of 200 MS/s. The total resulting bandwidth of the instrument is 0.5 MHz–100 MHz, without any relevant peaks in the amplitude profile (figure 2). Two tests were carried out. One with both specimens at room temperature (cold case) and one with the defect-free specimen preheated to a temperature of 80 °C (hot case).

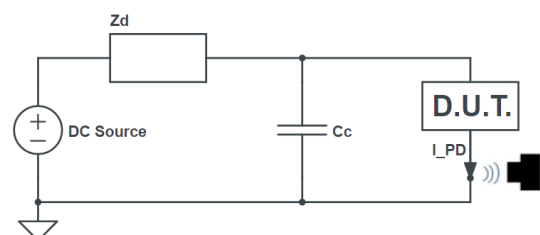


Fig. 1: Experimental setup.

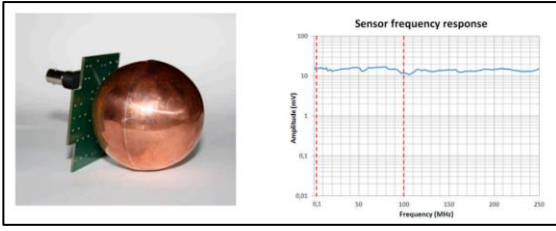


Fig. 2: UWB antenna sensor and frequency response in 0,1-100 MHz range.

### III. TIME-FREQUENCY MAP

After the measurement, the data were analyzed through the TF map. This technique uses the differences between time waveforms and frequencies spectra linked to PD pulses of different sources, to perform the separation of data in pattern distributed in a two-dimensional map in a similar way to PRPD but without requiring a phase reference. The split of data is carried out through the calculation of two quantities called: *Equivalent Time Length* (T) and *Equivalent Bandwidth* (F), described by the following equations:

$$T^2 = \int_{-\infty}^{+\infty} (t - t_0)^2 \cdot |\tilde{s}_i(t)|^2 dt \quad (1)$$

$$F^2 = \int_{-\infty}^{+\infty} (f - f_0)^2 \cdot |\tilde{S}_i(f)|^2 df \quad (2)$$

where  $\tilde{s}_i(t)$  is the normalized PD pulse (3),  $t_0$  (4) and  $f_0$  (5) are the temporal and spectral gravity centers respectively,  $\tilde{S}_i(f)$  is the Fourier transform of the normalized PD pulse (6). The normalization of the signal occurs through division by its own Euclidean norm. The calculation of all these quantities was implemented in MATLAB® environment.

$$\tilde{s}_i(t) = \frac{s_i(t)}{\sqrt{\int_{-\infty}^{+\infty} |s_i(t)|^2 dt}} \quad (3)$$

$$t_0 = \int_{-\infty}^{+\infty} t \cdot |\tilde{s}_i(t)|^2 dt \quad (4)$$

$$f_0 = \int_{-\infty}^{+\infty} f \cdot |\tilde{S}_i(f)|^2 df \quad (5)$$

$$\tilde{S}_i(f) = \int_{-\infty}^{+\infty} \tilde{s}_i(t) \cdot e^{-j2\pi ft} dt \quad (6)$$

Unlike many authors who assume that  $f_0$  is zero because, for a real signal, the spectrum is always symmetric about the origin, in this work a different approach was used. Neglecting the left side (negative) of the spectrum and doubling the positive frequency components to preserve the energy content of the original signal, it's possible to obtain a value for average frequency different from zero and therefore a greater amount of information about pulses [10]. Then for each detected pulse a couple of values (T, F) is determined.

In this way the information on the temporal waveforms and frequencies spectra is enclosed in a point positioned on a map. The advantage of this tool is that the data are analyzed using parameters that don't concern a single characteristic of the signal (amplitude, phase, time of occurrence, etc.) but a greater amount of information as the entire waveform and spectra are considered for their determination. PD pulses that sharing the same origin will arrange themselves in a specific region of the map, allowing a separation of different phenomena or noise rejection.

### IV. DENSITY-BASED CLUSTERING

A clustering algorithm was used to separate the data into homogeneous groups (cluster) to be analyzed separately with the aim of obtaining more information about the observed phenomena. The implemented technique is the *Density-Based Spatial Clustering of Applications with Noise* (DBSCAN) [11]. Proposed in 1996, it is one of the most popular clustering algorithms today used and cited in scientific literature. Cluster construction is based on the research of regions of points characterized by a density comparable to that established by the user. The algorithm requires two input parameters:

1. Radius of the Epsilon-Neighborhood of a point (Eps)
2. Minimum number of points inside the Epsilon-Neighborhood (MinPts)

Through these two inputs, the density of the clusters to be identified is fixed. Then, the algorithm proceeds by analyzing each point of the dataset and labeled them in three different ways as shown in figure 3.

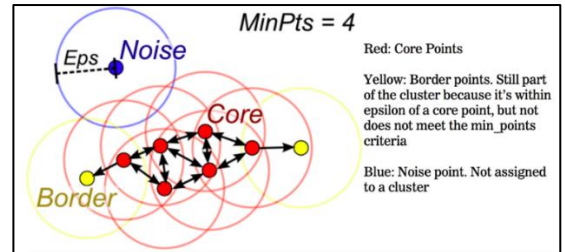


Fig. 3: Example of Density-Based Clustering.

Starting from a generic point  $P$  of the dataset, the code analyzes the number of points present within its Eps-neighborhood (included  $P$ ). Then the following condition is checked:

$$\text{Point inside the Eps\_Neighborhood} \geq \text{MinPts}$$

When this density condition is satisfied the points  $P$  is labeled as Core-Points (red) and represents the origin of a cluster. All the other point within his Eps-Neighborhood become part of the cluster. When the density condition isn't satisfied, but in the Eps-Neighborhood of point  $P$  there is a Core-Point,  $P$  is labeled as Border-Point (yellow). These points are located in the border region of the clusters. The last type are the Noise-Points (blue), located in regions where the density condition isn't satisfied, far from any Core-Point. The algorithm returns the final result after that all the points of the datasets have been labeled.

## V. RESULTS

### A. Cold Case

In this first case the measurement was performed keeping both specimens at room temperature. The test had a total duration of about 12 minutes in which two levels of HVDC voltage were applied (10 and 20 kV). From the trend of the repetition rate and the Time-Resolve-Partial-Discharge (TRPD) pattern, it's possible to observe the temporal evolution of the discharge phenomenon (figure 4). A rapid increase of the discharge activity is observed in the initial phase and after about 6 minutes from the start of the test. These phases correspond to variations in the supply voltage from 0 to 10 kV and from 10 to 20 kV. This effect can be attributed to the polarization current that is established when the voltage across a test specimen is switched on (dielectric polarization) and when it is switched off (dielectric depolarization) [12]. In the first case, once the steady state condition is reached, the discharge activity tends to decrease until it settles down to about ten discharges per minute. In the second case, the PD activity is more intense, a sign that the higher supply voltage stresses the material more. In figure 5 the TF map, clustered by DBSCAN, for the dataset acquired during cold case test is reported. A linear distribution is observed. The points are grouped in a single cluster by the DBSCAN algorithm. A small part of the points is instead dispersed. As expected, the latter have been labeled as Noise-Point. It has been verified that such impulses can be caused by external disturbances or by the presence of overlapping errors, i.e. the presence of several pulses in the same recording window. All pulses belonging to the main cluster (C1) show a waveform and spectrum typical of an internal discharge (figure 6).

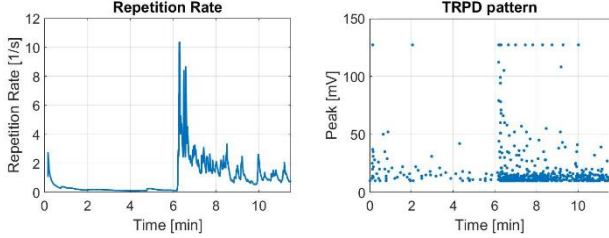


Fig. 4: Repetition rate and TRPD pattern for cold case measurement.

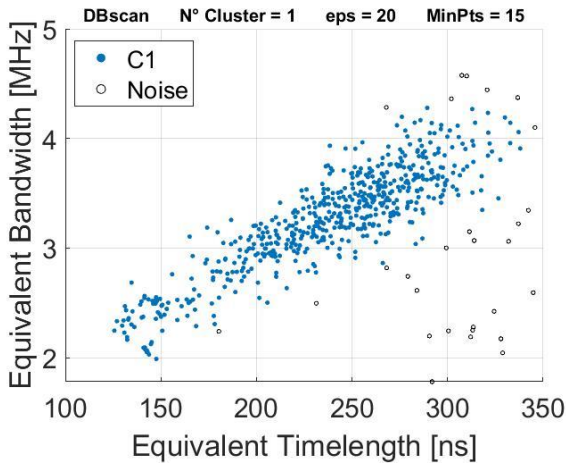


Fig. 5: TF map for dataset for cold case measurement.

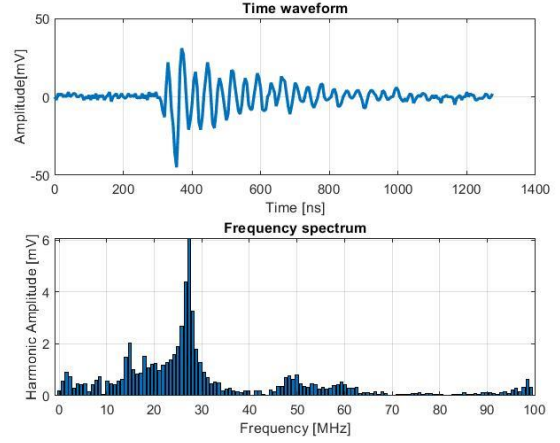


Fig. 6: Typical PD waveform and spectrum detected during cold case measurement for cluster (C1).

### B. Hot Case

During the second test a more intense PD activity was observed. It is believed that the increased discharge activity is due to the higher temperature of the defect-free specimen. In fact, the higher temperature leads also to a higher conductivity of the insulating layer. Consequently, the distribution of the voltage between the two specimens will be a function of the oil temperature variation. The test had a total duration of about 18 minutes in which three levels of HVDC voltage were applied (10, 15 and 20 kV). As for the cold case, in figure 7 the repetition rate and the TRPD pattern are reported. Also in this case, peaks of discharge activity are observed during the voltage increasing ramps. In figure 8 the TF map, clustered by DBSCAN, for the dataset acquired during hot case test is shown.

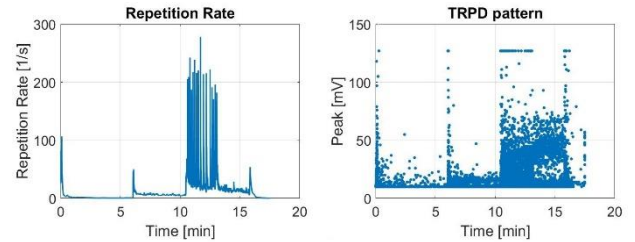


Fig. 7: Repetition rate and TRPD pattern for hot case measurement.

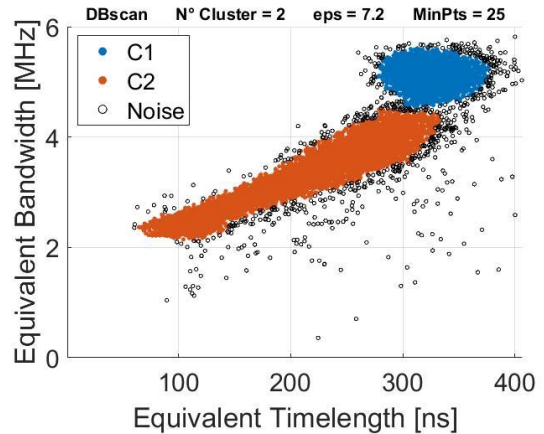


Fig. 8: TF map for dataset for hot case measurement

Two groups of data are shown, one with an almost linear distribution and a second one with a globular shape. Cluster C1 (blue) is formed by pulses that have waveforms and spectra like that shown in figure 9. Furthermore, from figure 11, it can be seen that these pulses peaks are all close to the trigger threshold (10 mV). Therefore, it is believed that these types of pulses are due to an external disturbance.

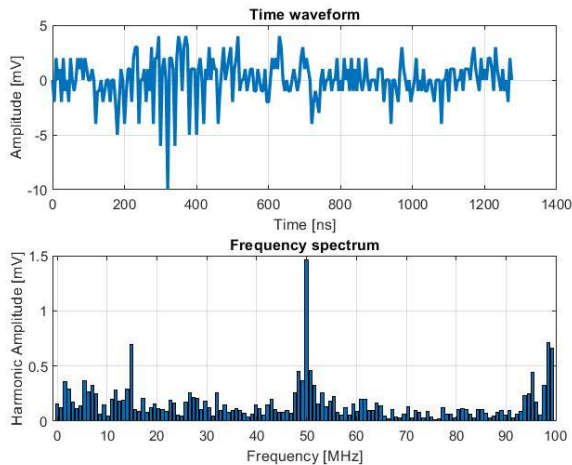


Fig. 9: Typical pulse waveform and spectrum for cluster C1 (blue) detected during hot case measurement.

Cluster C2 (orange) is formed by pulses that have waveforms and spectra like that shown in figure 10. Both in the time and frequency domains the trends are typical of those of internal discharges. The maximum frequency component is always between 20 and 30 MHz. From figure 11, it can be seen that these pulses peaks are distributed in a range from 10 mV to 127 mV. Therefore, through the time-frequency map it was possible to identify a subgroup of data, made up of partial discharge pulses, within a data set containing noise.

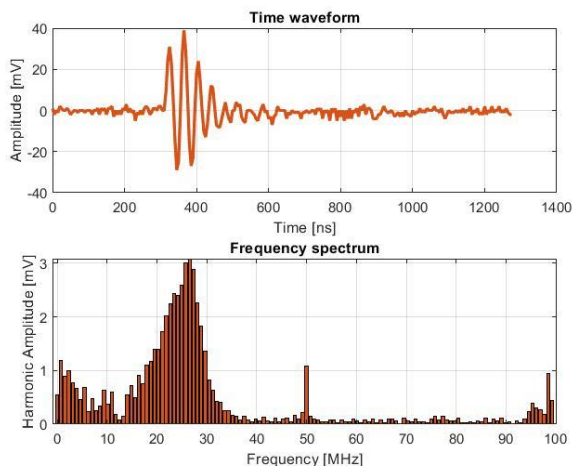


Fig. 10: Typical pulse waveform and spectrum for cluster C2 (orange) detected during hot case measurement.

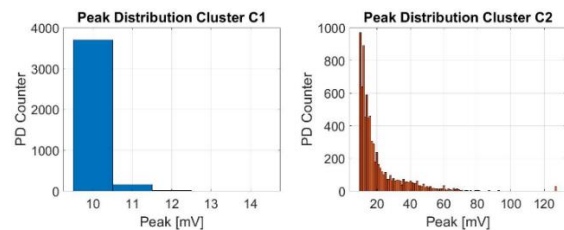


Fig. 11: Peak distributions of clusters C1 and C2.

## VI. CONCLUSION

The aim of this paper is to show how the TF map, combined with clustering algorithm, can be used for the analysis of PD measurement data under DC voltage, for which Phase Resolved Partial Discharges (PRPD) pattern cannot be available. With this approach it was possible to recognize and reject the noise due to external factors and analyze the PD pulses from different sources grouped in different clusters through DBSCAN algorithm.

## ACKNOWLEDGMENT

This work was realized with the co-financing from European Union – FSE, PON Research and Innovation 2014-2020 – DM 1062/2021.

## REFERENCES

- [1] S. Okabe, G. Ueta, H. Wada and H. Okubo, "Partial discharge-induced degradation characteristics of insulating materials of gas-filled power transformers," in *IEEE Transactions on Dielectrics and Electrical Insulation*, vol. 17, no. 6, pp. 1715-1723, Dec. 2010.
- [2] Imburgia, A.; Rizzo, G.; Romano, P.; Ala, G.; Candela, R. Time Evolution of Partial Discharges in a Dielectric Subjected to the DC Periodic Voltage. *Energies* 2022, 15, 2052.
- [3] Imburgia, A.; Romano, P.; Rizzo, G.; Viola, F.; Ala, G.; Chen, G. Reliability of PEA Measurement in Presence of an Air Void Defect. *Energies* 2020, 13, 5652.
- [4] Rizzo, G.; Romano, P.; Imburgia, A.; Viola, F.; Ala, G. The Effect of the Axial Heat Transfer on Space Charge Accumulation Phenomena in HVDC Cables. *Energies* 2020, 13, 4827.
- [5] P. Romano, A. Imburgia, G. Rizzo, G. Ala and R. Candela, "A New Approach to Partial Discharge Detection Under DC Voltage: Application to Different Materials," in *IEEE Electrical Insulation Magazine*, vol. 37, no. 2, pp. 18-32, March-April 2021.
- [6] P. Romano, G. Rizzo, C. Consolazione, R. Candela and G. Ala, "The Partial Discharge Behavior of Different Materials Under DC Periodic Stress," *2019 IEEE Conference on Electrical Insulation and Dielectric Phenomena (CEIDP)*, 2019, pp. 661-665.
- [7] J. C. Chan, H. Ma, and T. K. Saha, "Time-frequency sparsity map on automatic partial discharge sources separation for power transformer condition assessment," *IEEE Transactions on Dielectrics and Electrical Insulation*, vol. 22, no. 4, pp. 2271–2283, 2015.
- [8] R. Aldrian, G. C. Montanari, A. Cavallini et al., "Signal separation and identification of partial discharge in xlpe insulation under dc voltage," in *2017 1st International conference on electrical materials and power equipment (ICEMPE)*. IEEE, 2017, pp. 53–56. K. Elissa, "Title of paper if known," unpublished.
- [9] P. Romano, A. Imburgia, and G. Ala, "Partial discharge detection using a spherical electromagnetic sensor," *Sensors*, vol. 19, no. 5, 2019. [Online]. Available: <https://www.mdpi.com/1424-8220/19/5/1014>.
- [10] L. Cohen, *Time-frequency analysis*. Prentice hall New Jersey, 1995, vol. 778.
- [11] M. Ester, H.-P. Kriegel, J. Sander, X. Xu et al., "A density-based algorithm for discovering clusters in large spatial databases with noise." in *kdd*, vol. 96, no. 34, 1996, pp. 226–231.
- [12] P. Morshuis and J. Smit, "Partial discharges at dc voltage: their mechanism, detection and analysis," *IEEE Transactions on Dielectrics and Electrical Insulation*, vol. 12, no. 2.